Published in final edited form as:
J Biol Rhythms. 2000 April ; 15(2): 103–111.

Retinal Innervation of Calbindin-D_{28K} Cells in the Hamster Suprachiasmatic Nucleus: Ultrastructural Characterization

Damani N. Bryant[*], **Joseph LeSauter**[†], **Rae Silver**[†,‡,§], and **Maria-Teresa Romero**[*]

[*]Department of Psychology, Binghamton University, State University of New York, Binghamton, NY 13902, USA

[†]Department of Psychology, Barnard College, New York, NY 10027, USA

[‡]Department of Psychology, Columbia University, New York, NY 10027, USA

[§]Department of Anatomy and Cell Biology, College of Physicians and Surgeons, New York, NY 10032, USA

Abstract

The authors have described a subregion of the hamster hypothalamic suprachiasmatic nucleus (SCN) containing cells that are immunopositive for the cytosolic calcium-binding protein, Calbindin-D_{28K} (CaBP). Several lines of evidence indicate that this region may constitute the site of the pacemaker cells that are responsible for the regulation of circadian locomotor rhythms. First, 79% of the CaBP-immunoreactive (ir) neurons express Fos in response to photic stimulation, indicating that they are close to or part of the input pathway to pacemakers. Second, at the light microscopy level, retinal terminals innervate the CaBP subnucleus. Finally, destruction of this subnucleus renders animals arrhythmic in locomotor activity. In this study, the authors examined the ultrastructural relationship between cholera toxin (CTβ) labeled retinal fibers and the CaBP-ir subregion within the hamster SCN. CTβ-ir retinal terminals make primarily axo-somatic, symmetric, synaptic contacts with CaBP-ir perikarya. In addition, retinal terminals form synapses with CaBP processes as well as with unidentified profiles. There are also complex interactions between retinal terminals, CaBP perikarya, and unidentified profiles. Given that axo-somatic synaptic input has a more potent influence on a cell's electrical activity than does axo-dendritic synaptic input, cells of the CaBP subregion of the SCN are ideally suited to respond rapidly to photic stimulation to reset circadian pacemakers.

Keywords

calcium-binding proteins; calbindin-D_{28K}; CaBP; pacemaker; suprachiasmatic nucleus; retinal terminals; electron microscopy; circadian rhythms

---

The suprachiasmatic nucleus (SCN) of the hypothalamus is the site of the putative circadian clock in mammals (see Klein et al., 1991). The circadian system regulates the periodicity of many rhythmic responses in mammals including rest-wake cycles (see Moore-Ede et al., 1982), electrical activity, and neuropeptide levels (Inouye, 1996), to name a few. In the absence of exogenous stimuli, the circadian clock oscillates with a periodicity that is close to 24 h. The circadian timing system also has the capacity to entrain or synchronize the organism to the exogenous geo-solar cycle. The primary neural substrate responsible for the

---

Correspondence to: Maria-Teresa Romero.

transduction of exogenous photic stimuli is the retinohypothalamic tract (RHT), a monosynaptic pathway projecting from the retina to the SCN (Card and Moore, 1991; Moore, 1996). A secondary pathway, the geniculo-hypothalamic tract, also provides photic input to the circadian pacemaker. Photic information is integrated in the SCN to produce a stable phase relationship between physiological and behavioral activity and the environmental light-dark cycle (Meijer, 1991). While it is clear that the SCN is the site of the circadian pacemaker, the precise identity of retinorecipient cells that mediate entrainment remains to be elucidated.

We recently described cells immunopositive for Calbindin-D_{28K} (CaBP) in the caudal aspect of the hamster SCN (Silver et al., 1996). These cells form bilateral subnuclei, consisting of a tightly packed group of approximately 250 cells in each nucleus surrounded by an area devoid of CaBP immunoreactivity. Several lines of evidence indicate that cells in the region of the CaBP subnucleus may be circadian pacemakers, responsible for driving activity rhythms. Destruction of the CaBP-immunoreactive (ir) subnucleus disrupts locomotor rhythms in hamsters even when other parts of the SCN are spared (LeSauter and Silver, 1999a). Furthermore, transplantation studies suggest that recovery of function in SCN-lesioned hamsters is contingent upon the presence of CaBP-ir perikarya in the SCN grafts.

Another feature expected of the circadian pacemaker is the receipt of retinal input allowing pacemakers to be reset by light—directly or indirectly—thereby mediating the synchronization of the endogenous rhythm to light cues (Moore, 1996). There is some evidence that photic input reaches the CaBP perikarya: (1) Light exposure at circadian time (CT) 18 induces Fos protein expression in 79% of the CaBP-ir cells within the subnucleus; (2) Hamsters housed in constant darkness for 7 weeks show a significant increase in the number of CaBP-ir perikarya. This effect of housing in DD is more pronounced in *Tau* mutant hamsters (LeSauter et al., 1996b) and correlates with the greater phase-shifting effects of light in the mutant (Grosse et al., 1995). In summary, evidence from light-induced Fos, lesion, and transplantation studies is consistent with the suggestion that cells of the CaBP subregion are the locus of circadian pacemakers regulating entrained and free-running locomotor rhythms.

Double-label immunocytochemical analysis at the light microscopy (LM) level following intraocular injections of the tracer cholera toxin β subunit (CTβ) reveals that this subnucleus is densely innervated by CTβ-ir retinal terminals (Silver et al., 1996). This suggests that the subnucleus receives direct retinal input. The purpose of this study was to characterize, at the ultrastructural level, the nature of the retinal/CaBP appositions observed. Using double-label immunoelectron microscopy, we report primarily symmetric, axo-somatic synaptic contacts between retinal boutons and CaBP-ir neurons. Retinal synapses were also observed on CaBP-ir dendrites. Preliminary data from this study have been presented in abstract form (Bryant et al., 1996).

METHODS

Animals and Housing

Adult male hamsters (n = 8) were individually housed in translucent propylene cages (48 × 27 × 20 cm) equipped with a running wheel under light-dark conditions (14:10). Water and food were provided ad libitum. The room was maintained at an ambient temperature of 23 ± 2 °C. A white noise generator (91 spl) masked environmental noise.

Retinal Tract Tracing/Double-Label Immunocytochemistry

For retinal tract tracing, hamsters (n = 4) were anesthetized (sodium pentobarbital 100 mg/kg^{-1}) and injected intraocularly with 5 μl of 5% CTβ Subunit (List Biological, Campbell,

CA) 48 h prior to sacrifice. All hamsters received an overdose of anesthetic (sodium pentobarbital 200 mg/kg) and were subsequently perfused intracardially with 300–400 ml of 4% paraformaldehyde in 0.1 M phosphate buffer (PB). Brains were postfixed for 2 h at 4 °C. Forty micron coronal brain sections were cut on a DSK Microslicer (Ted Pella Inc., Redding, CA).

Double-label immunocytochemistry was performed using a modification of the procedure of Chen et al. (1990). Free-floating sections were rinsed in PB between each incubation step. Sections were first incubated in 0.3% hydrogen peroxide in PB. Sections were subsequently incubated in goat anti-choleragenoid antibody (1:10,000; List Biological, Campbell, CA) diluted in PB containing 1% normal rabbit serum (NRS), and 0.02% saponin (SAP; Sigma) at 4 °C for 48 h. Sections were subsequently incubated in biotinylated rabbit-anti-goat secondary antibody (1:200, Vector Labs, Burlingame, CA) in 0.02% PB/SAP for 1 h at room temperature. Immunoreactivity was visualized using the commercial avidin-biotin-HRP (1:200, Vector Labs) in 0.02% PB/SAP with 3′-3′ diaminobenzidine-1% glucose oxidase as the chromogen. Thoroughly rinsed sections were incubated in monoclonal anti-CaBP antibody (1:10,000; Sigma) in 0.02% PB/SAP containing 1% normal horse serum (NHS) and 1% NRS for 48 h at 4 °C. Sections were then incubated in biotinylated horse-anti-mouse antibody (1:200, Vector Labs) for 1 h at room temperature. To differentiate the second antigen at the ultrastructural level, avidin-biotin-HRP (1:200 Vector Labs) was used with the electron-dense chromogen tetramethylbenzidine (TMB) and ammonium heptamolybdate. TMB forms longitudinal crystal deposits on labeled structures. Briefly, sections were rinsed in PB, pH 6.0 and incubated in TMB-0.3% hydrogen peroxide for 20 min. Following another series of PB pH 6.0 rinses, sections were washed three times in tris pH 7.4. The TMB crystals were stabilized for 8–10 min in ice cold 3′-3′ diaminobenzidine-cobalt chloride solution, which produced a black reaction product.

Single-Label Immunocytochemistry

The brains of the remaining 4 hamsters were processed for single-label CaBP immunocytochemistry to characterize, in more detail, the ultrastructural features of CaBP cells in the absence of the deposits of TMB crystals. Animals were placed in dim red light for 1 week and perfused as described previously at CT 6 (n = 2) and CT 22 (n = 2) under sodium pentobarbital anesthesia (200 mg/kg). Free-floating 40 μm coronal sections were cut and immunocytochemically processed as described in the previous section using monoclonal anti-CaBP (1:10,000; Sigma). As before, immunoreactivity was visualized using the avidin-biotin HRP procedure using 3′-3′ diaminobenzidine-1% glucose oxidase as the chromogen.

Processing for Transmission Electron Microscopy (EM)

Both single- and double-labeled sections were prepared for EM as follows. The area of the SCN containing the CaBP-ir subnucleus was dissected from 40 micron sections and osmicated in 2% OsO4 containing 1.5% potassium ferricyanide for 1 h. Sections were dehydrated and flat embedded in EPON (Tousimis Research Corp., Rockville, MD). Blocks of resin were polymerized for 48 h at 60 °C. Semithin (0.75 μm) sections were cut on an LKB 2128 ultramicrotome and examined under LM to corroborate the presence of at least 4 CaBP positive cells to ensure that the cells observed were located in the CaBP subnucleus. Serial ultrathin sections (60 nm) were subsequently cut and placed on 300 × 300 copper grids. Ten to 50 consecutive sections were collected to analyze CaBP cells at various levels of sectioning. Ultrathin sections were examined under a Phillips 201 or Hitachi 7000 transmission electron microscope and photographed at magnifications between 1.5 K and 15 K.

Analysis of Double-Labeled Sections

Semithin sections (0.75 μm) were observed at the LM level to find at least 4–5 CaBP cells with CTβ-labeled retinal fibers in close apposition. Electron micrographs photographed from the chosen ultrathin sections were examined for the following: CTβ axons synapsed on CaBP soma (axosomatic); CTβ synapses on CaBP dendrites (axo-dendritic); CaBP/CaBP synapses (axo-axonal, axo-dendritic, and axo-somatic); CTβ terminals synapsed on nonlabeled dendrites, perikarya, or axons; and any possible neural-glial contact. Synapses or synaptic active zones were identified by visual confirmation of the presence of several structures including (1) a synaptic cleft, (2) pre- and/or postsynaptic specialization, and (3) the presence of synaptic vesicles in the presynaptic element (Peters et al., 1991).

Quantitative Analysis

The surface area of CaBP-ir cells was estimated as follows. The plasmalemmal and nuclear membrane were traced from electron micrographs into Minicad for Macintosh (Diehl's Graphsoft, Columbia, MD) using a WACOM Tablet (Wacom Technology Corp., Vancouver, WA) adjusting for print magnification. The cross-sectional surface area of the plasmalemmal and/or nuclear profiles was subsequently calculated using Minicad. Only labeled cells sectioned through the nucleus were measured.

RESULTS

Light Microscopy

As described previously (Silver et al., 1996), the CaBP-ir subnucleus is located in the third quarter of the hamster SCN surrounded by an area devoid of CaBP-ir structures. CTβ-ir retinal fibers course through the retinorecipient area of the SCN, which includes the CaBP-ir subnucleus (Fig. 1) and extends dorsally beyond the borders of the SCN (see also Aïoun et al., 1998). The density of retinal fibers is particularly high at the level of the CaBP-ir region. Examination of semithin sections (0.75 μm) indicates that varicose CTβ-ir fibers are in close apposition to CaBP-ir perikarya, as well as to unidentified perikarya (Fig. 2).

Ultrastructural Analysis

Morphology of CaBP-ir Structures—A total of 78 CaBP-ir cells (21 cells in single-labeled material and 57 in double-labeled material) were sampled in this study. Single-labeled CaBP material was used to examine the morphological characteristics of CaBP-ir structures in the SCN. The estimated cross-sectional surface area of CaBP cells within the SCN is 141.4 ± 56.2 μm^2 while the estimated nuclear cross-sectional area is 78.7 ± 35.3 μm^2. The large variability in cell size is a consequence of the random orientation of CaBP-ir cells in coronal sections through the SCN. At the levels sampled, CaBP-ir nuclei were very large, encompassing, on average, 45% to 60% of the total cellular cross-sectional area (Fig. 3a) and containing one or two nucleoli. Nonlabeled cells in the areas sampled seemed to exhibit a similar nucleus to cell surface area ratio. CaBP perikarya in the SCN are fusiform, with euchromatic nuclei, which typically display at least one large invagination and several smaller invaginations. Numerous mitochondria are observed in the cytoplasm of CaBP cells. Rough endoplasmic reticulum and golgi apparati are not abundant, consistent with the scant cytoplasm these cells contain. In some cases, the organelles were concentrated on one pole of the cell exhibiting abundant cytoplasm. CaBP-ir cells were frequently observed close to other CaBP neurons (Fig. 3a, 3b). Unidentified membranes, possibly glia, were interposed (with few exceptions) between adjacent CaBP-ir profiles. CaBP-ir glia were not observed in any of the sections collected.

Morphology of CTβ-ir Retinal Terminals—At the ultrastructural level, CTβ-ir retinal structures, visualized with DAB as the chromogen, exhibited an electron-dense globular appearance. Retinal terminals contained mitochondria and abundant clear-cored synaptic vesicles aggregated near the active zone. No lucent mitochondria were observed in CTβ-ir terminals.

Retinal Terminals Synapse on CaBP-ir Perikarya—CTβ-ir retinal terminals containing clear-cored synaptic vesicles formed symmetric synapses with CaBP-ir perikarya (Fig. 4) as indicated by the presence of pre- and postsynaptic specializations and a synaptic cleft. Appositions between CTβ-ir retinal terminals and CaBP-ir cells had "synapselike" characteristics in a large percentage of the profiles examined (Fig. 5). In many instances, it was difficult to determine the exact nature of these appositions because of the intense immunolabel that obscured synaptic morphology.

CaBP-ir Processes and CTβ-ir Retinal Terminals Synapse on Other CaBP Perikarya and Dendrites—Complex synaptic interactions were frequently observed between CaBP-ir dendritic profiles, CaBP-ir perikarya, and CTβ-ir retinal terminals. In Figure 5, for example, a CaBP-ir neuron receives synaptic input from both a retinal terminal and a CaBP terminal within a 5 μm distance of each other on the perikaryal membrane. Complex appositions between CTβ-ir terminals and CaBP dendritic profiles were also observed (Fig. 6), suggesting that there is an elaborate interaction between retinal axons and CaBP-ir dendrites.

Retinal Terminals and CaBP-ir Processes Synapse on Unidentified Structures—CTβ-ir retinal terminals formed axo-dendritic, axo-axonal, and axo-somatic contacts (Figs. 7 and 8) with unidentified profiles. In some cases, a single retinal terminal contacted more than one postsynaptic element.

DISCUSSION

The results of the present study indicate that retinal terminals form primarily axo-somatic, symmetrical synapses with CaBP-ir neurons in the hamster SCN. Additionally, CaBP-ir axons form synaptic profiles with other CaBP-ir perikarya and dendrites, indicating that these structures are reciprocally innervated. Although most retinal-CaBP synapses are axo-somatic, axo-dendritic synaptic interactions were also observed.

We systematically examined the neuropil surrounding CaBP-ir neurons, we observed very few axo-dendritic retinal contacts on CaBP-ir profiles. Given that axo-somatic synapses can, in general, exert a more powerful influence on the electrical potential of the entire neuron (Burke, 1998), the presence of a large percentage of axo-somatic retinal contacts on CaBP-ir cells suggests that photic input probably has a potent effect on the electrical activity of these cells.

It is also interesting to note that lucent mitochondria were not observed in the retinal terminals of the hamster material, consistent with the description of Aïoun et al. (1998). This finding contrasts with data from the rat and mouse where retinal terminals are characterized by the presence of lucent mitochondria and make predominantly axo-dendritic and asymmetrical synapses (Guldner, 1978a, 1978b; Card and Moore, 1991; Castel et al., 1993; Tanaka et al., 1997). It should be noted that axo-somatic symmetrical retinal synapses have also been described in these species.

Given that the retinorecipient area of the hamster SCN is more extensive than the CaBP-ir subnucleus, it is clear that other neuronal subpopulations within the SCN also receive retinal

input. Consistent with this fact, we observed a large number of unidentified neuronal profiles that form synaptic specializations with retinal terminals. Furthermore, it also seems likely that some neuronal subpopulations within the SCN are preferentially innervated by retinal terminals in either an axo-somatic or axo-dendritic manner. We found primarily axo-somatic retinal input on CaBP-ir neurons in the hamster, while Aïoun et al. (1998) and Tanaka et al. (1997) demonstrate predominantly axo-dendritic retinal synaptic profiles on GRP-ir neurons in the hamster and rat SCN, respectively. It is interesting to note that Aïoun et al. (1998) did not observe any synaptic contacts between retinal fibers and vasoactive intestinal polypeptide (VIP)-ir neurons in the hamster SCN. This contrasts with data from the rat, where retinal terminals form both axo-dendritic and axo-somatic synaptic contacts with VIP-ir neurons in the SCN (Ibata et al., 1989; Tanaka et al., 1993). The data suggest that the ultrastructural morphology of retinal input into the SCN varies with “peptidergic phenotype” in various rodent species.

In addition to characteristic interactions with retinal terminals, it seems likely that several peptidergic subpopulations in the SCN may have a modulatory role in entrainment. For instance, in the rat, it has been suggested that VIP-ir and GRP-ir structures code the duration of the light phase (direct retinal input) while NPY input (indirect retinal input) codes the transition from the light phase to the dark phase and vice versa (Shinohara et al., 1993; Tanaka et al., 1997). Assuming that the primary and secondary retinal inputs have analogous roles in the hamster and rat SCN, the CaBP-ir subnucleus is in an ideal anatomical location to receive unprocessed as well as precoded information about environmental photic conditions and relay it to other structures. It has been demonstrated that GRP-ir (hamster) and VIP-ir neurons (hamster, rat, and mouse) SCN express the immediate early gene *c-fos* in response to photic stimulation (Romijn et al., 1996; Aïoun et al., 1998; Castel et al., 1998). While some of these subpopulations receive direct retinal input (axo-somatic or axo-dendritic), others, such as VIP-ir neurons in the hamster, might be activated in an indirect manner (axo-axonal input onto dendritic processes; see Fig. 8 for an example). Ongoing studies will characterize the ultrastructural relationship between CaBP-ir neurons and other subpopulations in the hamster SCN to determine the context in which the CaBP-ir subnucleus operates.

The implications of a structure immunoreactive for a calcium binding protein as the putative master circadian pacemaker merit further consideration, given the role of calcium in the circadian timing system. First, there is extensive experimental evidence in support of the idea that glutamate (GLU) is the primary neurotransmitter of the RHT (Castel et al., 1993; van den Pol and Dudek, 1993; Ebling, 1996). Furthermore, photic signals are thought to be conveyed to the SCN via ionotropic N-methyl-D-aspartate (NMDA) and non-NMDA GLU receptors (Shibata et al., 1994). Excitatory amino acids, including GLU, are known to transiently increase intracellular calcium concentrations in cultured SCN neurons via activation of GLU receptors in the SCN (van den Pol et al., 1992) even in the presence of tetrodotoxin (TTX) in vitro (Tominaga et al., 1994). Given that infusion of TTX, a sodium channel blocker, into the SCN in vivo disrupts photic entrainment and behavioral expression of drinking rhythms, without affecting timekeeping (Schwartz, 1991), it seems likely that the individually oscillating clock cells (Welsh et al., 1995) might be synchronized in a calcium-dependent manner. Calcium concentrations are thus maintained at appropriate levels, at least in part, by cytosolic calcium-binding proteins, which are believed to passively limit the rise in intracellular free calcium concentrations (Baimbridge et al., 1992). Assuming that the biological clock oscillates in a calcium-dependent manner, it is prudent to buffer such a structure against excessive calcium levels. Furthermore, another calcium-binding protein, calretinin, is found in the mouse (Abrahamson and Moore, 1998) and rat (Speh and Moore, 1997) SCN. The implications of a protective mechanism mediated by calcium-binding

proteins are profound, as synchronization to the geo-solar day is important for ecological and evolutionary reasons.

Acknowledgments

This work was supported by the Research Foundation of SUNY (MTR) and N537119 (R5). We thank Henry Eichelberger and David Tuttle for technical assistance. We are grateful to Dr. A.-J. Silverman for her invaluable comments on a previous version of this manuscript.

References

Abrahamson EE, Moore RY. The organization of the mouse suprachiasmatic nucleus (SCN): Immunocytochemical analysis of retinal innervation and cell and fiber distribution. Soc Res Biol Rhythms Abstr. 1998; 6:83.

Aïoun J, Chambille I, Peytevin J, Martinet L. Neurons containing gastrin releasing peptide and vasoactive intestinal polypeptide are involved in the reception of the photic signal in the suprachiasmatic nucleus of the Syrian hamster: An immunocytochemical ultrastructural study. Cell Tissue Res. 1998; 291:231–253. [PubMed: 9426310]

Baimbridge KG, Celio MR, Rogers JH. Calcium-binding proteins in the nervous system. Trends Neurosci. 1992; 15:303–308. [PubMed: 1384200]

Bryant DN, LeSauter J, Silver R, Romero M-T. Retinal synapses on calbindin-ir cells in the hamster suprachiasmatic nucleus: A double label immunoelectron microscopy study. Soc Neurosci Abstr. 1996; 22:1140.

Burke, RE. Spinal cord: Ventral horn. In: Shepherd, GM., editor. The Synaptic Organization of the Brain. Oxford University Press; New York: 1998. p. 77-120.

Card, JP.; Moore, RY. The organization of visual circuits influencing the circadian activity of the suprachiasmatic nucleus. In: Klein, DC.; Moore, RY.; Reppert, SM., editors. Suprachiasmatic Nucleus: The Mind's Clock. Oxford University Press; New York: 1991. p. 51-76.

Castel M, Belenky M, Cohen S, Ottersen OP, Storm-Mathiesen J. Glutamate-like immunoreactivity in retinal terminals of the mouse suprachiasmatic nucleus. Eur J Neurosci. 1993; 5:361–381.

Castel M, Belenky M, Cohen S, Wagner S, Schwartz WS. Light-induced *c-Fos* expression in the mouse suprachiasmatic nucleus: Immunoelectron microscopy reveals co-localization in multiple cell types. Eur J Neurosci. 1998; 9:1950–1960. [PubMed: 9383218]

Chen W-P, Witkin JW, Silverman AJ. Sexual dimorphism in the synaptic input to gonadotropin releasing hormone neurons. Endocrinology. 1990; 126:695–702. [PubMed: 2137080]

Ebling FJP. The role of glutamate in the photic regulation of the suprachiasmatic nucleus. Prog Neurobiol. 1996; 50:109–132. [PubMed: 8971980]

Grosse J, Louden ASI, Hastings MH. Behavioural and cellular responses to light of the circadian system of *Tau* mutant and wild type Syrian hamsters. Neuroscience. 1995; 65:587–597. [PubMed: 7777171]

Guldner FH. Synapses of optic nerve afferents in the rat suprachiasmatic nucleus: I. Identification, qualitative description, development and distribution. Cell Tissue Res. 1978a; 194:17–35. [PubMed: 719729]

Guldner FH. Synapses of optic nerve afferents in the rat suprachiasmatic nucleus: II. Structural variability as revealed by morphometric examination. Cell Tissue Res. 1978b; 194:36–54.

Ibata Y, Takahashi Y, Okamura H, Kawakami F, Terubayashi H, Kubo T, Yanaihara N. Vasoactive intestinal polypeptide (VIP)-like immunoreactive neurons located in the rat suprachiasmatic nucleus receive a direct retinal projection. Neurosci Lett. 1989; 97:1–5. [PubMed: 2918990]

Inouye, S-I. Circadian rhythms of neuropeptides in the suprachiasmatic nucleus. In: Buijs, RM.; Kalsbeek, A.; Romijn, HJ.; Pennartz, CMA.; Mirmiran, M., editors. Progress in Brain Research. Vol. 3. Elsevier Science; Amsterdam: 1996. p. 75-90.

Klein, DC.; Moore, RY.; Reppert, SM. Suprachiasmatic nucleus: The mind's clock. Oxford University Press; New York: 1991.

LeSauter J, Silver R. Localization of a suprachiasmatic nucleus subregion regulating locomotor rhythmicity. J Neurosci. 1999a; 19:5574–5585. [PubMed: 10377364]

LeSauter J, Silver R, Stevens H, Jansen H, Lehman MN. Calbindin expression in the hampster SCN is influenced by photic conditions. NeuroReport. 1996b; 10:3159–3163. [PubMed: 10574553]

Meijer, JH. Integration of visual information by the suprachiasmatic nucleus. In: Klein, DC.; Moore, RY.; Reppert, SM., editors. Suprachiasmatic Nucleus: The Mind's Clock. Oxford University Press; New York: 1991. p. 107-120.

Moore, RY. Entrainment pathways and the functional organization of the circadian system. In: Buijs, RM.; Kalsbeek, A.; Romijn, HJ.; Pennartz, CMA.; Mirmiran, M., editors. Progress in Brain Research. Vol. 3. Elsevier Science; Amsterdam: 1996. p. 103-119.

Moore-Ede, MC.; Sulzman, FM.; Fuller, CA. The Clocks That Time Us: Physiology of the Circadian Timing System. Harvard University Press; Cambridge, MA: 1982.

Peters, A.; Palay, SL.; Webster, HD. The Fine Structure of the Nervous System: Neurons and Their Supporting Cells. Oxford University Press; New York: 1991.

Romijn HJ, Sluiter AA, Pool CW, Wortel J, Buijs RM. Differences in colocalization between Fos and PHI, GRP, VIP and VP in neurons of the rat suprachiasmatic nucleus after a light stimulus during the phase delay versus the phase advance period of the night. J Comp Neurol. 1996; 372:1–8. [PubMed: 8841917]

Schwartz WJ. Further evaluation of the tetrodotoxin-resistant circadian pacemaker in the suprachiasmatic nuclei. J Biol Rhythms. 1991; 6:149–158. [PubMed: 1663409]

Shibata S, Watanabe A, Hamada T, Ono M, Watanabe S. N-methyl-D-aspartate induces phase shifts in circadian rhythm of neuronal activity in the rat SCN *in vitro*. Am J Physiol. 1994; 36:R360–R364. [PubMed: 7520671]

Shinohara K, Tominaga K, Isobe Y, Inouye S-I. Photic regulation of peptides in the ventrolateral subdivision of the suprachiasmatic nucleus of the rat: Daily variations of vasoactive intestinal polypeptide, gastrin releasing peptide and neuropeptide Y. J Neurosci. 1993; 13:793–800. [PubMed: 8426236]

Silver R, Romero M-T, Besmer HR, Leak R, Nunez JM, LeSauter J. Calbindin-D_{28K} cells in the hamster SCN express light-induced Fos. NeuroReport. 1996; 7:1224–1228. [PubMed: 8817537]

Speh JC, Moore RY. Fos expression in calretinin (CAR) neurons of the rat suprachiasmatic nucleus (SCN). Soc Neurosci Abstr. 1997; 23:511.

Tanaka M, Hyashi S, Tamada Y, Ikeda T, Hisa Y, Takamatsu T, Ibata Y. Direct retinal projections to GRP neurons in the suprachiasmatic nucleus of the rat. Neuro-Report. 1997; 8:2187–2191.

Tanaka M, Ichitani Y, Okamura H, Tanaka Y, Ibata Y. The direct retinal projection to VIP neuronal elements in the rat SCN. Brain Res Bull. 1993; 31:637–640. [PubMed: 8518955]

Tominaga K, Geusz ME, Michel S, Inouye S-I. Calcium imaging in organotypic cultures of the rat suprachiasmatic nucleus. NeuroReport. 1994; 5:1901–1905. [PubMed: 7841372]

van den Pol AN, Dudek FE. Cellular communication in the circadian clock, the suprachiasmatic nucleus. Neuroscience. 1993; 56:793–811. [PubMed: 7904331]

van den Pol AN, Finkbeiner SM, Cornell-Bell AH. Calcium excitability and oscillations in suprachiasmatic nucleus neurons and glia *in vitro*. J Neurosci. 1992; 12:2648–2664. [PubMed: 1351936]

Welsh DK, Logothetis DE, Meister M, Reppert SM. Individual neurons dissociated from rat suprachiasmatic nucleus express independently phased circadian firing rhythms. Neuron. 1995; 14:697–706. [PubMed: 7718233]

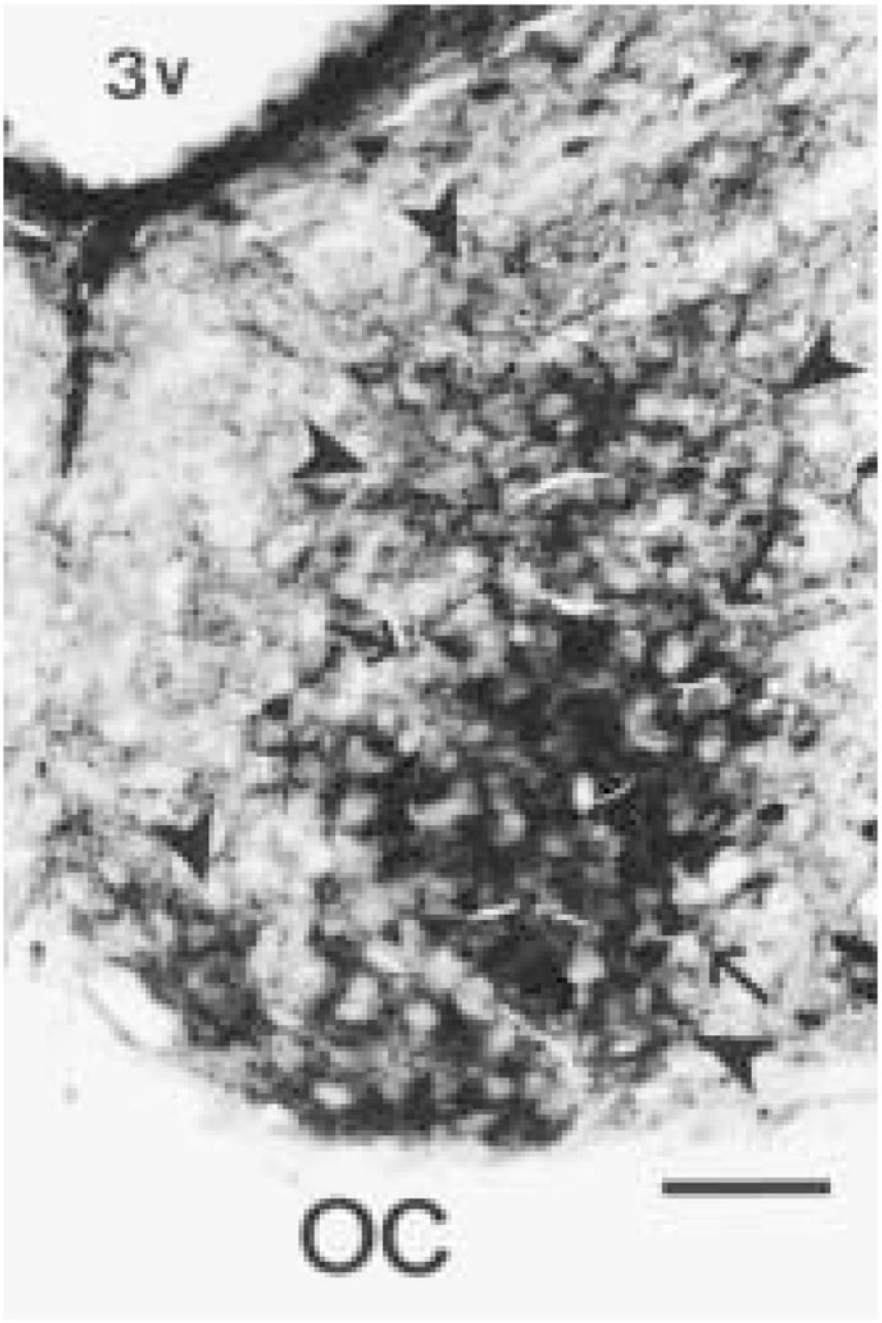

Figure 1.
Photomicrograph of the unilateral hamster SCN double labeled for cholera toxin β subunit (CTβ) and Calbindin-D_{28K} (CaBP) at the light microscopy level. CTβ-immunoreactive (ir) retinal terminals are observed throughout the SCN (arrow heads). The CaBP-ir subnucleus (arrows) is surrounded by an area devoid of CaBP-ir structures. 3v = third ventricle. Magnification bar = 100 μm.

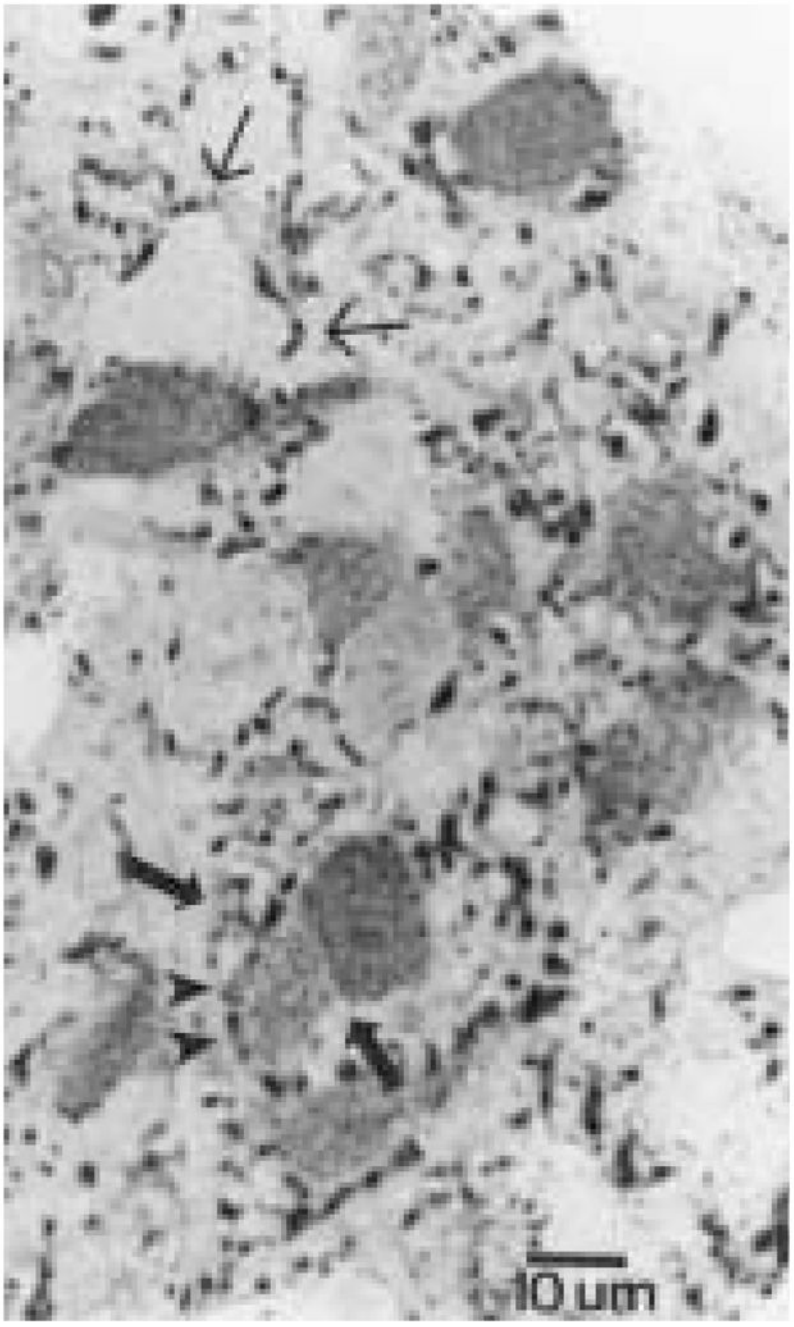

Figure 2.
Micrograph of a semithin section (0.75 μm) depicting several Calbindin-D_{28K} (CaBP)-immunoreactive (ir) cells surrounded by cholera toxin β subunit (CTβ)-ir fibers. Two CaBP-ir cells are observed close to each other (large arrows). A CTβ-ir fiber partially encircles one of the CaBP-ir cells (arrowheads). Non-identified perikarya are also encircled by retinal terminals, which are also abundant in the neuropil (small arrows). Magnification bar = 10 μm.

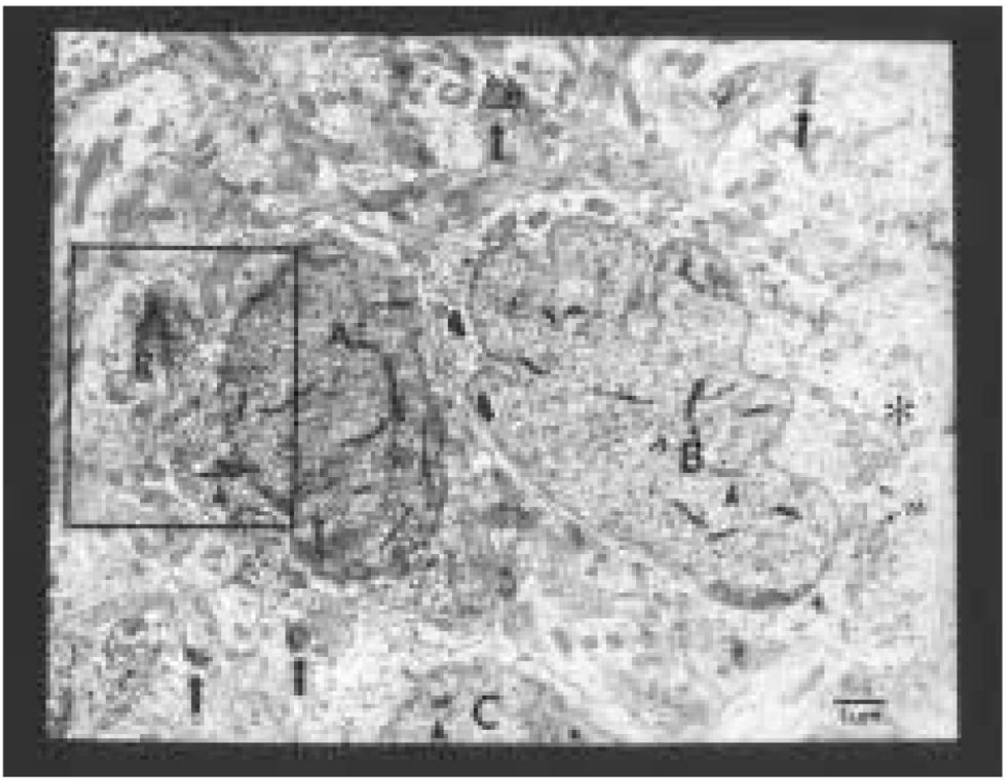

Figure 3a.

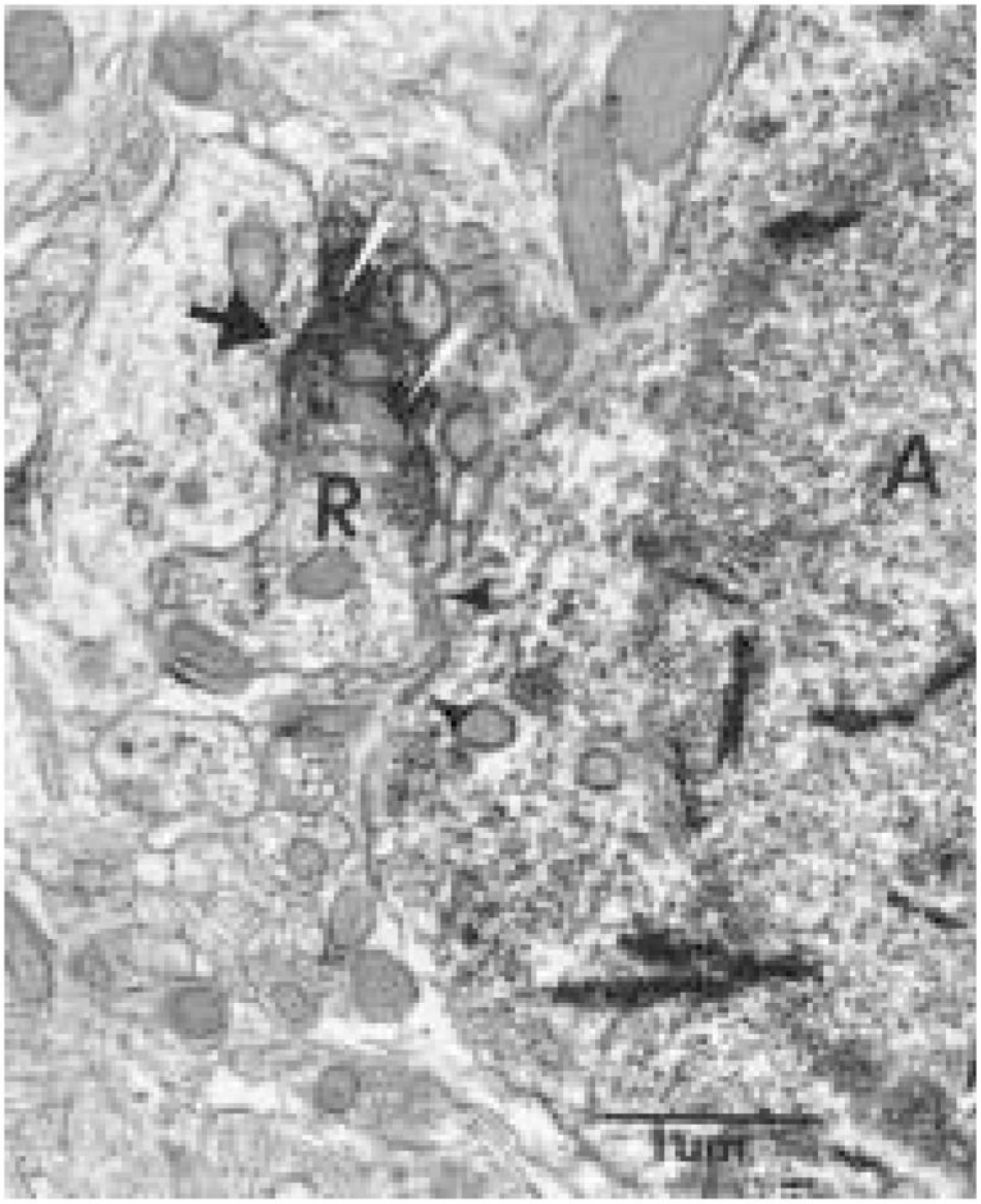

Figure 3b.

Figure 3.

Figure 3a. A cluster of three Calbindin-D_{28K}-immunoreactive (ir) neurons (A, B, C), indicated by the presence of tetramethylbenzidine crystals (arrowheads), lie close to each other. Unidentified membranes (black and white arrow heads), possibly glia, are interposed between neurons (A) and (B). These cells also have large invaginated nuclei, occupying most of the cross-sectional surface area. The perikaryon of cell (B) contains numerous mitochondria (M) and golgi apparatus (asterisk). A cholera toxin β subunit (CTβ)-ir terminal (R) is also close to cell (A). The neuropil contains small profiles of retinal axons in passage (arrows). Magnification = × 18,500.

Figure 3b. An enlargement of the cholera toxin β subunit (CTβ)-immunoreactive retinal terminal in proximity to cell (A) described in Fig. 3a. This terminal is not uniformly

immunolabeled. While a few synaptic vesicles can be discerned in the intensely labeled portion of the terminal (white arrows), there appear to be no vesicles in the lightly labeled portion of the terminal. The retinal terminal synapses (large arrow) on an unidentified dendrite but not on the Calbindin-D_{28K} neuron (arrow heads). Magnification = × 40,500.

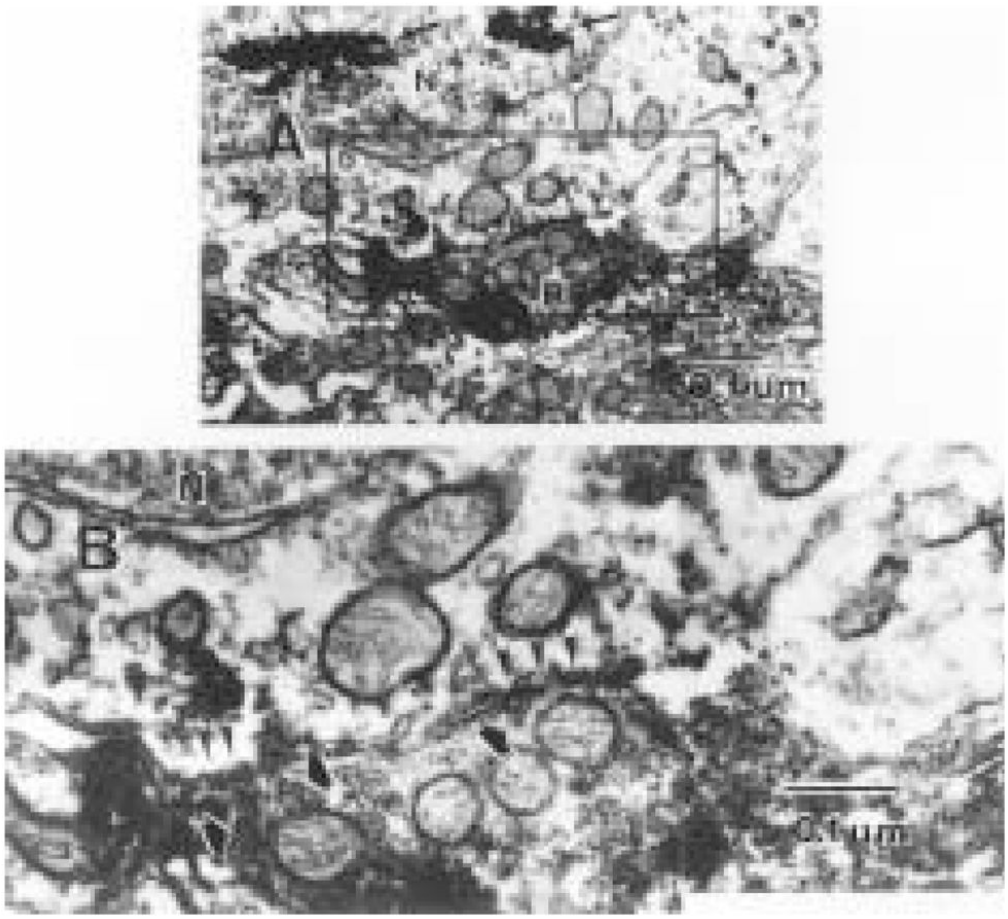

Figure 4.

(A) A cholera toxin β subunit (CTβ)-immunoreactive (ir) retinal terminal synapses on the perikaryal membrane of a Calbindin-D_{28K}-ir cell, indicated by the presence of tetramethylbenzidine crystals in the nucleus (arrows). Numerous mitochondria are observed on both the presynaptic and postsynaptic sides of the synaptic profile (magnification = × 34,000). At higher magnification (B), two postsynaptic enlargements (arrow heads) are visible near each other. Synaptic vesicles (black/white arrows) are present in the presynaptic profile near each synapse, although they are partially obscured by the intense immunolabel. Magnification = × 97,000.

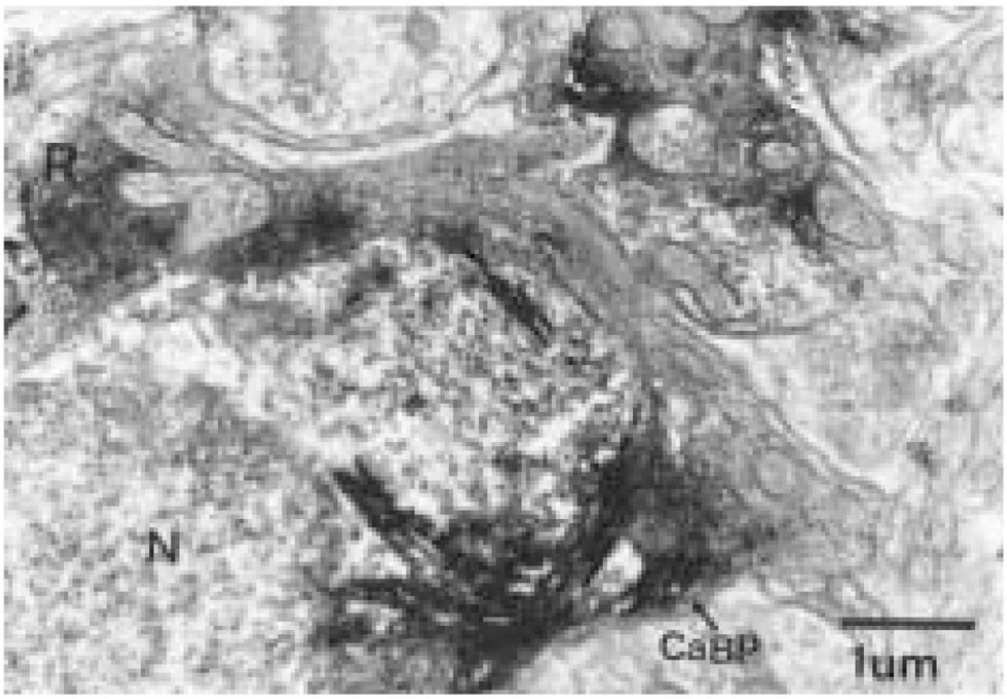

Figure 5.

A Calbindin-D_{28K} (CaBP)-immunoreactive (ir) neuron receives two axo-somatic appositions, one from a retinal terminal (R) and the other from a CaBP-ir fiber. The electron-dense TMB reaction product used to identify CaBP profiles makes it difficult to discern synaptic vesicles or a synaptic cleft between the CaBP-ir neuron and CaBP terminal. However, the presence of a cleft and synaptic vesicles is more apparent in the active zone of the retinal terminal as opposed to that of the CaBP-ir. Magnification = × 22,000.

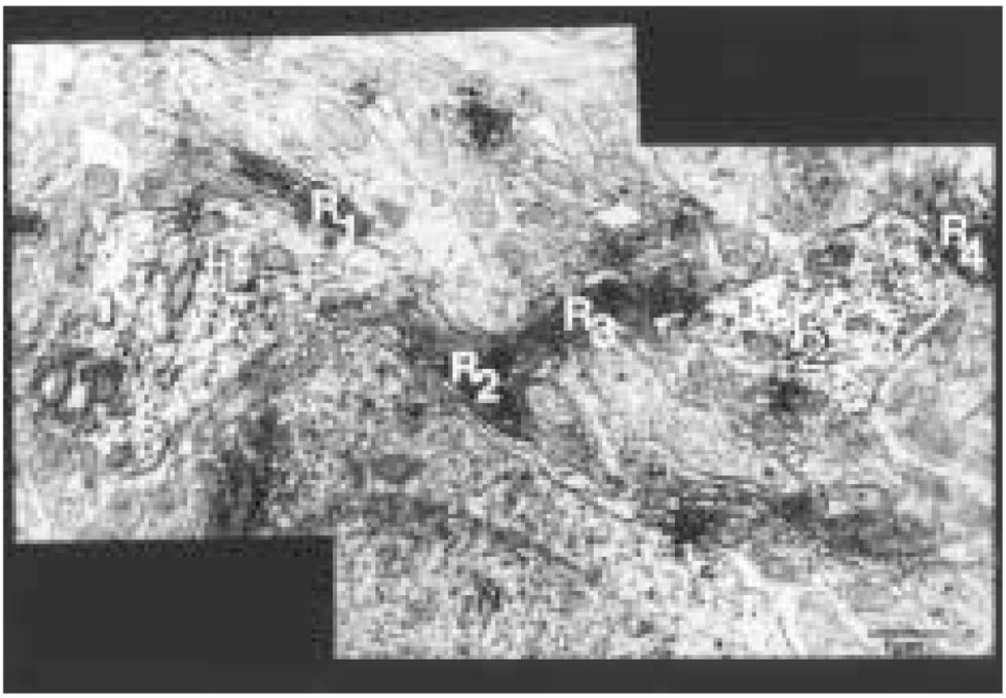

Figure 6.
Four longitudinally sectioned cholera toxin β subunit (CTβ)–immunoreactive (ir) axons of passage (R_1-R_4) surround considerable portions of Calbindin-D_{28K} (CaBP) dendrites (T_1 and T_2). This type of arrangement is found throughout the neuropil of the CaBP subnucleus. Magnification = × 30,000.

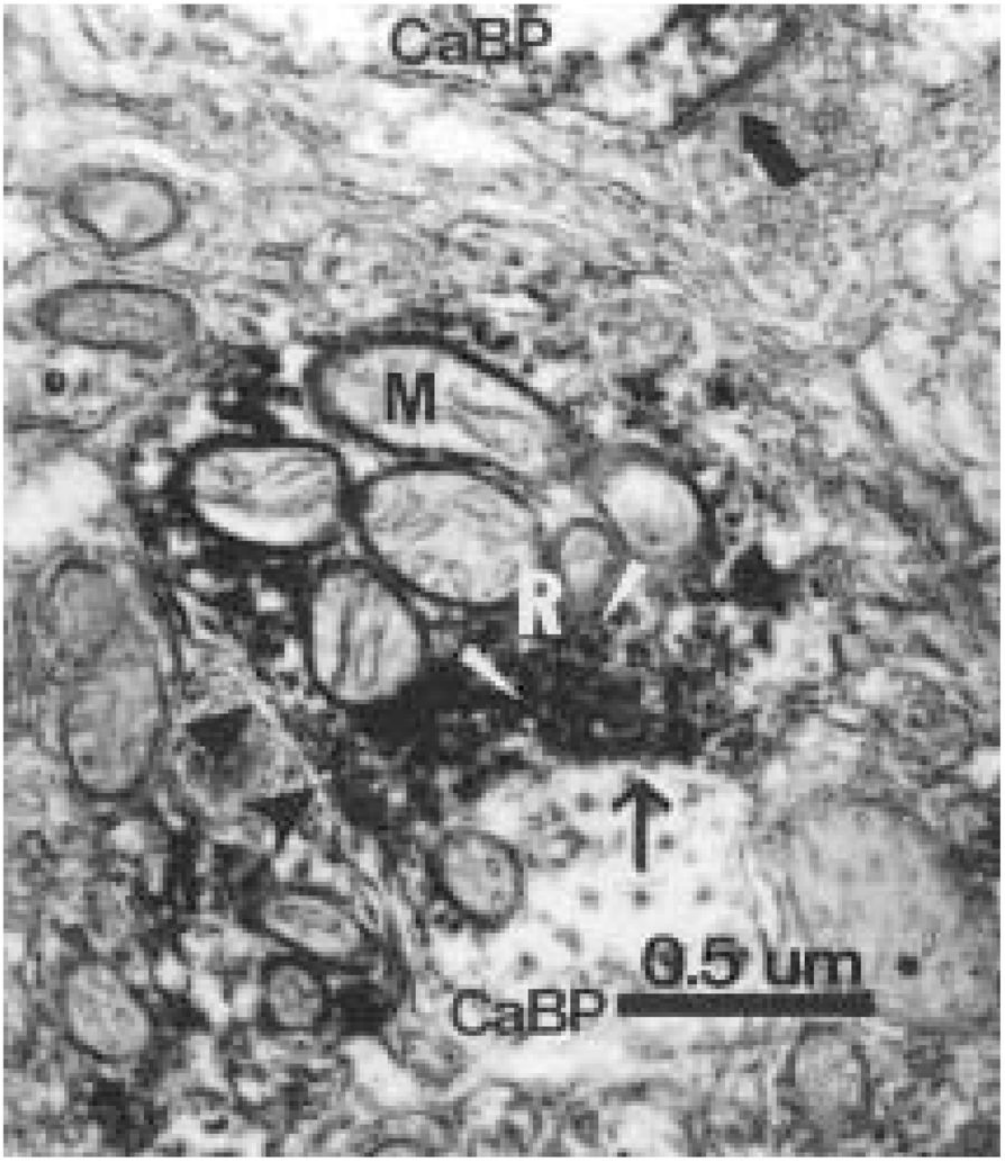

Figure 7.

A cholera toxin β subunit–immuonoreative (ir) retinal terminal (R) forms a synaptic contact with a Calbindin-D_{28K} (CaBP) dendritic profile (arrow). The retinal terminal (R) contains numerous mitochondria (M) and synaptic vesicles (white arrowheads). The retinal bouton and CaBP-ir terminal are partially enclosed by unidentified membranes, which are possibly glia (arrowheads). This photomicrograph also depicts a nonidentified axonal bouton forming a symmetrical axo-somatic synapse with a CaBP-ir profile (large arrow). Magnification = × 54,000.

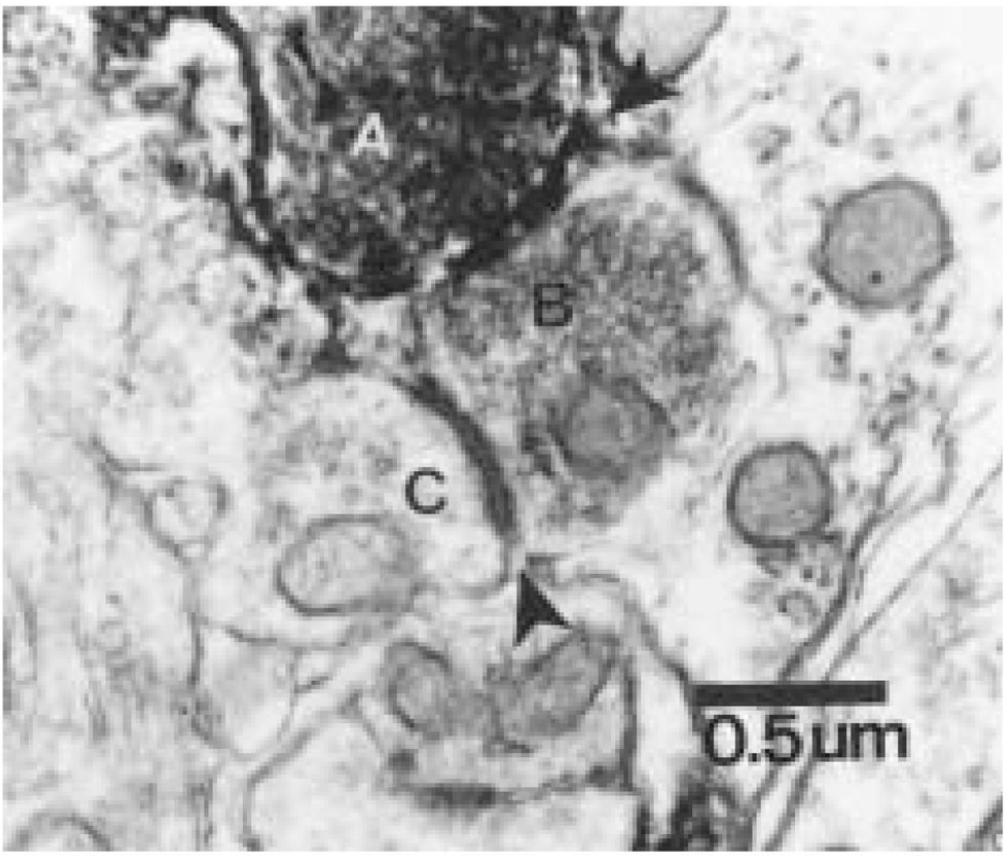

Figure 8.
A cholera toxin β subunit–immuonoreative retinal terminal (A) synapses with an unidentified axonal profile (B), which contains numerous synaptic vesicles. This profile in turn synapses on another unidentified dendritic profile (C). This complex interaction suggests that axo-axonal retinal input modulates the response of SCN neurons to light in both a direct and indirect manner. Magnification = × 40,000.